Observation of O^+ ^4P-$^4D^0$ lines in proton aurora over Svalbard

N. Ivchenko,[1,2] M. Galand,[3] B. S. Lanchester,[1] M. H. Rees,[1] D. Lummerzheim,[4] I. Furniss,[5] and J. Fordham[5]

Received 17 December 2003; revised 18 March 2004; accepted 26 March 2004; published 29 May 2004.

[1] Spectra of a proton aurora event show lines of O^+ ^4P-$^4D^0$ multiplet (4639–4696 Å) enhanced relative to the $N_2^+1N(0,2)$ compared to normal electron aurora. Conjugate satellite particle measurements are used as input to electron and proton transport models, to show that *p*/H precipitation is the dominant source of both the O^+ and N_2^+1N emissions. The emission cross-section of the multiplet in *p* collisions with O and O_2 estimated from published work does not explain the observed O^+ brightness, suggesting a higher emission cross-section for low energy *p* impact on O. *INDEX TERMS:* 0310 Atmospheric Composition and Structure: Airglow and aurora; 2407 Ionosphere: Auroral ionosphere (2704); 2419 Ionosphere: Ion chemistry and composition (0335); 2455 Ionosphere: Particle precipitation. **Citation:** Ivchenko, N., M. Galand, B. S. Lanchester, M. H. Rees, D. Lummerzheim, I. Furniss, and J. Fordham (2004), Observation of O^+ ^4P-$^4D^0$ lines in proton aurora over Svalbard, *Geophys. Res. Lett.*, *31*, L10807, doi:10.1029/2003GL019313.

1. Introduction

[2] The ultimate source of auroral emissions is precipitation of energetic particles into the atmosphere. The auroral spectrum depends on the composition of the upper atmosphere, and the type and energy distribution of the precipitating particles. Doppler-shifted atomic hydrogen lines [e.g., *Lanchester et al.*, 2003] are the unique signature of *p* precipitation, and are emitted by the energetic H atoms produced by charge exchange in the *p* beam. Various other spectral features seen in electron aurora are observed in proton aurora as well [*Galand et al.*, 2002], excited both by direct *p*/H impact and by secondary e^-.

[3] An important auroral diagnostic emission of $N_2^+1N(1,3)$ is blended with the O^+ ^4P-$^4D^0$ multiplet (4638–4696 Å). Recently the O^+ lines were studied in electron aurora, and their emission cross-section was estimated [*Ivchenko et al.*, 2004, and references therein]. The multiplet is emitted in the transition between $2s^22p^23p^4D^0$ and $2s^22p^23s^4P$ levels (Figure 1). We present a case study of proton aurora, combining ground-based spectral measurements with conjugate satellite particle measurements. We show that the observed O^+ multiplet brightness cannot be due to e^- excitation. Excitation in collisions with *p* and H is discussed, leading to the conclusion that reported cross-sections of *p* processes are not sufficient alone to produce the observed O^+ brightness.

2. Spectrographic Imaging Facility

[4] The Spectrographic Imaging Facility (SIF) is a suite of optical instruments, located at the auroral station (78.2°N, 15.8°E) near Longyearbyen, Svalbard. A description of the SIF is given by *McWhirter et al.* [2003], and data reduction techniques are described by *Ivchenko et al.* [2004]. Here we use data from the High Throughput Imaging Echelle Spectrograph (HiTIES) [*Chakrabarti et al.*, 2001]. The field of view is defined by a slit covering 8° centered on the magnetic zenith. By using high orders high spectral resolution is achieved. The overlapping orders are separated by a mosaic of interference filters placed at the image plane of the light diffracted from the grating. In the data used here, three spectral intervals were selected containing the H_β, $N_2^+1N(0,2)$ and $N_2^+1N(1,3)$. The data were acquired with the MIC detector [*Fordham et al.*, 1991]. We believe the absolute calibration uncertainties to be below 50%. The presented spectra are integrated over the central 2° of the slit. The spectral resolution is 1 Å and integration time 30 sec.

3. December 15, 2001 Event

[5] On December 15, 2001 solar wind number densities were above 50 cm^{-3} between 14:00 and 17:00 UT, while the IMF B_z stayed positive (ACE satellite data not shown). These conditions were favourable for intense *p* precipitation at high magnetic latitudes. Intense H_β emission (over 100 R) was measured by the SIF in the dusk auroral oval during the time of high solar wind density. The DMSP F-14 satellite overflew the auroral station (closest approach of the magnetic footprint to the station was at 17:02 UT; see Figure 2). LLBL-type precipitation was measured by the satellite between 17:01:20 UT and 17:03:40 UT. The energy spectra of electrons and protons for the time of the closest conjunction were used as input to the respective transport models. Most of the precipitating energy flux is carried by protons (0.4 mW m^{-2}), with two peaks at characteristic energies of just below 1 keV and about 8 keV. Electron energy flux of under 0.1 mW m^{-2} is carried by electrons with energies below 0.3 keV.

[6] The time history of SIF spectra is presented in Figure 3. The top panel is dominated by the O^+ lines at 4649.1 Å and 4641.8 Å, with the weaker feature at 4652 Å being the head of the $N_2^+1N(1,3)$ band, which is degraded towards the blue. The second panel shows the spectrum of the H_β emission from energetic H, Doppler broadened and

[1]School of Physics and Astronomy, University of Southampton, UK.
[2]Also at Alfvén Laboratory, Royal Institute of Technology, Stockholm, Sweden.
[3]Center for Space Physics, Boston University, Boston, Massachusetts, USA.
[4]Geophysical Institute, University of Alaska Fairbanks, Fairbanks, Alaska, USA.
[5]Department of Physics and Astronomy, University College, London, UK.

0094-8276/04/2003GL019313$05.00

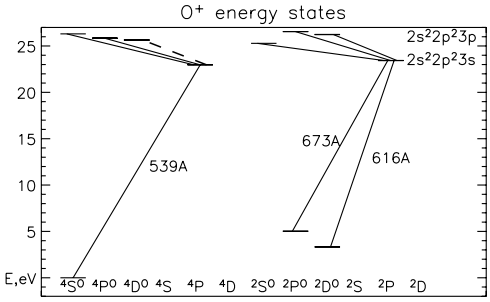

Figure 1. Energy diagram of O^+ with $O^{++}(^3P)$ core. The ^4P-$^4D^0$ multiplet is dashed.

shifted towards shorter wavelengths (coming downward). The bottom panel shows the $N_2^+1N(0,2)$ band, with the head at 4709 Å and degraded to the blue.

[7] Figure 4 shows the spectrum at the time of conjunction. It differs noticeably from a typical electron aurora spectrum that is also shown. The grey curve is the fitted background spectrum. Besides the continuum, it contains weak contributions from N_2 first positive and Vegard-Kaplan bands [*Sivjee*, 1980]. After subtracting the background, the brightnesses can be estimated. For N_2^+ 1N(0,2) integration over the observed spectral range yields about 10 R, which is an underestimate, since part of the R branch extends further into the blue. Using the method described by *Ivchenko et al.* [2004] we obtain 13 R for the 1N(0,2). Table 1 lists this value together with the observed brightnesses of O^+ ^4P-$^4D^0$ multiplet and H_β, 11.9 R and 102 R respectively.

[8] *Ivchenko et al.* [2004] found that the O^+ ^4P-$^4D^0$ brightness in electron aurora is on average 0.1 of $N_2^+1N(0,2)$. Modelling showed that the maximum ratio of the emissions does not exceed 0.5, a value only reached for electrons with energies of several 100 eV. In our case the O^+ and N_2^+ 1N(0,2) brightnesses are nearly equal.

[9] The quality of the data is compromised by the hazy sky conditions. However, apart from enhancements of the background due to variations in the haze, seen in all panels between 15 UT and 16 UT, and between 18:20 UT and 18:50 UT, the brightness variations are rather smooth in time. The DMSP F-14 data suggest a large spatial scale of *p* precipitation. The thin cloud cover has two effects - it reduces intensities in the field of view because of stronger extinction, but also it scatters emissions generated elsewhere into the instrument aperture [*Gattinger et al.*, 1991]. This makes the interpretation of the absolute intensities difficult if small transverse scales are present in the auroral display. However, we believe that in our case the aurora was uniform on scales larger than the field of view of the spectrograph, so that the scattering would mainly result in lower intensities. As the measured features are all within a small wavelength range, the same extinction factor applies and the relative brightnesses are unaffected.

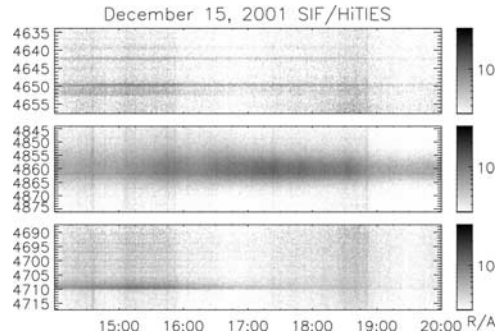

Figure 3. Spectra taken between 14:00 UT and 20:00 UT on December 15, 2001. Geocoronal emission is visible at the unshifted H_β wavelength (4861.3 Å).

4. Modelling the Emissions

[10] Particle data from the DMSP F-14 satellite can be used to predict the individual contributions of various processes to the brightnesses of the emissions observed.

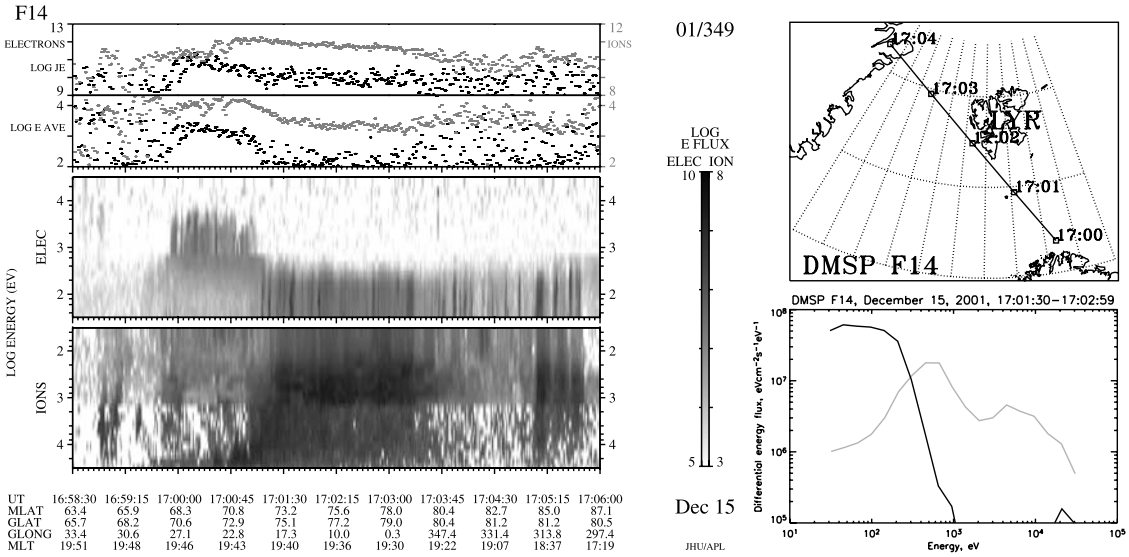

Figure 2. Electron and ion data from DMSP F-14 satellite. Top panels - energy flux (ev/cm^2/s) and characteristic energy (eV) of precipitating electrons and ions. Bottom panel - differential energy flux (eV/(cm^2 s sr ev)) of electrons and ions. Top right: DMSP F14 magnetic footprint at 100 km (triangle and LYR mark the auroral station). Bottom right: proton (grey) and electron (black) energy spectra at the conjunction.

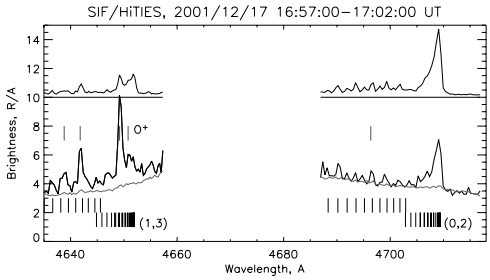

Figure 4. Spectrum of the N_2^+1N bands and O^+ lines at the time of conjunction. Thin grey line is the background spectrum (see text). Vertical lines mark position of the O^+ lines and the rotational lines of the P and R branches of the N_2^+ (0,2) and (1,3) bands. The upper curve is an electron aurora spectrum (17:02 UT on Dec 17, 2001), reduced by a factor of 25, and shifted upward for clarity.

The N_2^+ and O^+ emissions can be excited in electron, proton and energetic hydrogen collisions.

[11] We model the contribution from the electron precipitation using a transport model by *Lummerzheim and Lilensten* [1994], and the O^+ emission cross sections from *Ivchenko et al.* [2004]. The modelled brightnesses are summarized in Table 1. Electron precipitation produces no H_β. The brightness of N_2^+ 1N(0,2) excited in e^- collisions is 1.75 R, and that of the O^+ multiplet is 0.5 R.

[12] The transport of the precipitating p and H is a complicated process, because protons capture electrons in charge exchange processes, becoming hydrogen atoms; and energetic hydrogen atoms lose electrons in stripping processes. Thus, a pure p or H precipitation on its way down through the atmosphere becomes a mixed p/H beam. We use a code which solves the coupled transport equations for p and H [*Galand et al.*, 1997], including the collisional angular redistribution as described by *Lanchester et al.* [2003]. Given an incident p flux, it predicts the H emission Doppler profiles, auroral emission rates (when the emission cross section is known) and ion production rates. It also calculates the source function of the secondary electrons (the proto-electrons) produced in the proton beam. The integrated brightness of H_β at the time of the conjunction is 255 R (see Table 1). This is higher than the observed value, indicating strong extinction due to the haze. An atmospheric extinction coefficient for the clear conditions was estimated by *Lummerzheim et al.* [1990] to be 1.49. To reconcile the model with the data, a further factor of 1.7 is needed, which is reasonable for hazy conditions.

[13] The 1N bands of N_2^+ are also excited in p/H collisions with N_2. We assume the set of cross sections for production of the N_2^+ 1N(0,0) band as used in the model [*Galand et al.*, 1997], and Franck-Condon factors, which give the 1N(0,2) brightness of 17.7 R. Finally, the source function of proto-electrons obtained from the proton transport code is used as an input to the electron transport code to give N_2^+ 1N(0,2) and O^+ ^4P-$^4D^0$ intensities of 1 R and 0.01 R respectively.

[14] It is clear from Table 1 that the electron impact processes contribute very little to the O^+ ^4P-$^4D^0$ brightness. The p precipitation is responsible for the dominant part of the emissions in the observed spectral intervals. Assuming the extinction of 2.5, the observed N_2^+ 1N(0,2) is ca 60% brighter than modelled, which is a good agreement considering the uncertainties involved.

5. Excitation of the O^+ Lines by p/H Impact

[15] The brightness of O^+ lines due to the e^- precipitation is an order of magnitude below the observed. Excitation by the protoelectrons is negligible, because of the very fast fall-off of their energy spectra, leaving only a small part of the population above the threshold for $O^{+4}D^0$ state excitation (39.3 eV). This leaves most of the emissions unaccounted for by the e^- excitation.

[16] The O^+ lines are excited in p/H impact on O and O_2:

$$p + \mathrm{O} \rightarrow \mathrm{O}^+ + (\mathrm{p} + \mathrm{e}, \mathrm{H}) \quad (1)$$

$$\mathrm{H} + \mathrm{O} \rightarrow \mathrm{O}^+ + (\mathrm{H} + \mathrm{e}, \mathrm{p} + 2\mathrm{e}) \quad (2)$$

$$p + \mathrm{O}_2 \rightarrow \mathrm{O}^+ + \mathrm{O} + (\mathrm{p} + \mathrm{e}, \mathrm{H}) \quad (3)$$

$$\mathrm{H} + \mathrm{O}_2 \rightarrow \mathrm{O}^+ + \mathrm{O} + (\mathrm{H} + \mathrm{e}, \mathrm{p} + 2\mathrm{e}) \quad (4)$$

There are very few studies of excitation of high lying states of O^+ in p/H collisions. *Wilhelmi and Schartner* [2000] studied UV and visible fluorescence from O and O_2 in p impact, and published emission cross-sections for the 539 Å emission for p energies above 17 keV. This line originates from the lower state of the ^4P-$^4D^0$ multiplet (see Figure 1), which is populated, along with direct excitation, by cascading from $3p$ ($^4S^0$,$^4P^0$,$^4D^0$) states. The cascading is significant, as $3p \rightarrow 3s$ transitions (including ^4P-$^4D^0$) are readily seen in the visible fluorescence spectrum. Thus, this 539 Å cross-section is the upper limit for the ^4P-$^4D^0$ emission cross-section. In a recent theoretical study *Kirchner et al.* [2000] calculated the cross section for excitation of $O^+(3p\ ^{2,4}P)$ in equation (1) for p energies above 1 keV using the basis generator method in the framework of the independent particle model. This cross-section includes all $3p\ ^{2,4}P$ states: the six in Figure 1 and other states with excited O^{++} core. Even though the cross-section does not include cascading from higher levels, it is clearly the upper limit of the ^4P-$^4D^0$ emission cross-section. Both cross-sections are shown in Figure 5. We used the cross-section of *Kirchner et al.* [2000] (log-log extrapolated below 1 keV) for processes (1) together with the modelled altitude profile of p intensities to estimate the upper limit of 4.1 R for the brightness of the O^+ multiplet. We also made a

Table 1. Observed and Modelled Emissions for the Event

Brightness [R]	H_β	1N(0,2)	O^+
SIF observation 17:02 UT	102	13.0	11.9
Modelled (no extinction)			
Electron precipitation	0.0	1.75	0.5
p/H precipitation	254.9	17.65[a]	0.6–3[b]
Proto-electrons	0.0	1.0	0.01

[a]Estimated from 1N(0,0) using the Franck-Condon factors.
[b]Estimated range - see text.

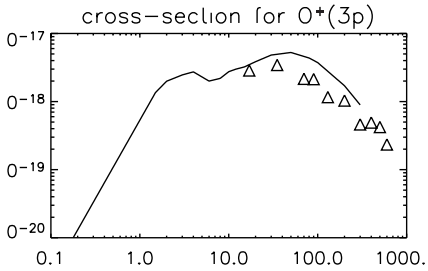

Figure 5. Cross-section for production of O^+ in $3p$ state, calculated by *Kirchner et al.* [2000] (extrapolation below 1 kev). Triangles - experimental cross-section for 539Å line for p impact on O [*Wilhelmi and Schartner*, 2000].

calculation taking the cross-section below 1 keV equal to that at 1 keV (rather than extrapolating). The predicted upper limit to ^4P-$^4D^0$ brightness from equation (1) only increased to 4.7 R. An estimate of the brightness produced in process (3) can be obtained by using twice the cross-section for p + O, resulting in 2.2 R. These values should be decreased by a ratio of ^4P-$^4D^0$ brightness to the total brightness of all $3p \rightarrow 3s$ transitions. We speculate that this ratio is at least 0.1, but probably does not exceed 0.5. Thus, a brightness of the order of 1 R is to be compared to the observed value of 12 R, which in turn should be increased to account for extinction (see discussion above). This means that the published cross-sections for the p processes alone cannot account for the observed brightness.

[17] It is useful to consider the total production rate of O^+ in the proton transport model. The total column production rate of $2.56 \cdot 10^9$ $cm^{-2}s^{-1}$ is dominated by process (1), contributing $2.0 \cdot 10^9$ $cm^{-2}s^{-1}$ (90% being due to electron capture). Process (2) amounts to $3.6 \cdot 10^8$ $cm^{-2}s^{-1}$, and processes (3) and (4) to $1.1 \cdot 10^8$ $cm^{-2}s^{-1}$ and $0.84 \cdot 10^8$ $cm^{-2}s^{-1}$ respectively. Observations suggest a column emission rate of over 20 R, which is $2 \cdot 10^7$ photons $cm^{-2}s^{-1}$. Processes (3) and (4) cannot be responsible for this rate, since this would imply that 10% of O^+ ions produced by dissociative processes are in the $3p^4D^0$ state, which is too much to be realistic. Thus, either up to 1% of O^+ produced in p collisions with O emit the ^4P-$^4D^0$ multiplet, or it is emitted by up to 5% of O^+ ions resulting from H impact on O. The former is more plausible, but still implies that the cross-section of equation (1) is significantly larger than assumed above. Assuming the experimental data of *Wilhelmi and Schartner* [2000] are reliable, cross-sections below 17 keV are the likely cause for the disagreement. With the total cross-section for electron capture in p + O collisions being almost constant for p energies below 10 keV at 10^{-15} cm^2 [*Hamre et al.*, 1999], the branching of 1% as discussed above implies ^4P-$^4D^0$ emission cross-section of ca 10^{-17} cm^2 for that energy range, which is difficult to reconcile with the calculations by *Kirchner et al.* [2000].

6. Summary

[18] In the presented event p precipitation is the dominant source of the N_2^+ 1N and O^+ ^4P-$^4D^0$ emissions. Modelled H_β and N_2^+ 1N brightnesses are consistent with the observations, allowing for extinction due to the hazy conditions. The ratio of the O^+ ^4P-$^4D^0$ multiplet to the N_2^+ 1N(0,2) band is enhanced in proton aurora compared to normal electron aurora. The existing ionization-$3p$-excitation cross-section, together with the modelled p intensities, put an upper limit on the predicted ^4P-$^4D^0$ brightness, which is an order of magnitude below the observed value. To explain the observed brightnesses, about 1% of all produced O^+ ions must emit a ^4P-$^4D^0$ photon. Electron capture and ionization by p collisions with O are the dominant processes for O^+ production in the event. Emission cross-section of the order of 10^{-17} cm^2 for p energies below 10 keV would be consistent with the observations.

[19] **Acknowledgments.** MG is supported by NASA grant NAG5-12773. The DMSP particle detectors were designed by D. Hardy of AFRL, and data obtained from JHU/APL. We thank D. Hardy, F. Rich, and P. Newell for its use.

References

Chakrabarti, S., D. Pallamraju, J. Baumgardner, and J. Vaillancourt (2001), HiTIES: A high throughput imaging echelle spectrograph for ground-based visible airglow and auroral studies, *J. Geophys. Res.*, *106*, 30,337–30,348.

Fordham, J. L., et al. (1991), MIC photon counting detector, *Proc. SPIE Int. Soc. Opt. Eng.*, *1449*, 87–98.

Galand, M., J. Lilensten, W. Kofman, and R. B. Sidje (1997), Proton transport model in the ionosphere: 1. Multistream approach of the transport equations, *J. Geophys. Res.*, *102*, 22,261–22,272.

Galand, M., D. Lummerzheim, A. Stephan, B. Bush, and S. Chakrabarti (2002), Electron and proton aurora observed spectroscopically in the far ultraviolet, *J. Geophys. Res.*, *107*(A7), 1129, doi:10.1029/2001JA000235.

Gattinger, R. L., A. Vallance Jones, J. H. Hecht, D. J. Strickland, and J. Kelly (1991), Comparison of ground-based optical observations of N2 second positive to N2 (+) first negative emission ratios with electron precipitation energies inferred from the Sondre Stromfjord radar, *J. Geophys. Res.*, *96*, 11,341–11,351.

Hamre, B., et al. (1999), Cross sections for capture, excitation and ionization in proton-oxygen collisions, *J. Phys. B: At. Mol. Opt. Phys.*, *32*, L127–L131.

Ivchenko, N., et al. (2004), Observations of O^+ (^4P-$^4D^0$) lines in electron aurora over Svalbard, *Ann. Geophys.*, in press.

Kirchner, T., et al. (2000), Quantum-mechanical description of ionization, capture, and excitation in proton collisions with atomic oxygen, *Phys. Rev. A*, *61*, doi:10.1103/052710.

Lanchester, B. S., et al. (2003), High resolution measurements and modelling of aurora hydrogen emission line profiles, *Ann. Geophys.*, *21*, 1629–1643.

Lummerzheim, D., and J. Lilensten (1994), Electron transport and energy degradation in the ionosphere: Evaluation of the numerical solution, comparison with laboratory experiments and auroral observations, *Ann. Geophys.*, *12*, 1039–1051.

Lummerzheim, D., et al. (1990), The application of spectroscopic studies of the aurora to thermospheric neutral composition, *Planet. Space Sci.*, *38*, 67–78.

McWhirter, I., et al. (2003), A new spectrograph platform for auroral studies in Svalbard, *Proc. Atmos. Stud. Opt. Methods*, *92*, 73–76.

Sivjee, G. G. (1980), Anomalous vibrational distribution of N2/+/1 NG emissions from a proton aurora, *J. Geophys. Res.*, *85*, 206–212.

Wilhelmi, O., and K.-H. Schartner (2000), Proton and electron impact on molecular and atomic oxygen: I. High resolution fluorescence spectra in the visible and VUV spectral range and emission cross-sections for dissociative ionisation and excitation of O_2, *Eur. Phys. J. D*, *11*, 79–90.

J. Fordham and I. Furniss, Department of Physics and Astronomy, University College, London, WC1E 6BT, UK.

M. Galand, Center for Space Physics, Boston University, Boston, MA 02215, USA.

N. Ivchenko, B. S. Lanchester, and M. H. Rees, School of Physics and Astronomy, University of Southampton, Southampton, SO17 1BJ, UK.

D. Lummerzheim, Geophysical Institute, University of Alaska Fairbanks, Fairbanks, AK 99775-7320, USA.